IMMUNOLOGY

A hierarchy of affinities between cytokine receptors and the common gamma chain leads to pathway cross-talk

Pauline Gonnord,*† Bastian R. Angermann,*‡ Kaitlyn Sadtler,§¶ Erin Gombos,‖ Pascal Chappert,** Martin Meier-Schellersheim,††‡‡ Rajat Varma††‡‡§§

Cytokines belonging to the common gamma chain (γ_c) family depend on the shared γ_c receptor subunit for signaling. We report the existence of a fast, cytokine-induced pathway cross-talk acting at the receptor level, resulting from a limiting amount of γ_c on the surface of T cells. We found that this limited abundance of γ_c reduced interleukin-4 (IL-4) and IL-21 responses after IL-7 preexposure but not vice versa. Computational modeling combined with quantitative experimental assays indicated that the asymmetric cross-talk resulted from the ability of the "private" IL-7 receptor subunits (IL-7Rα) to bind to many of the γ_c molecules even before stimulation with cytokine. Upon exposure of T cells to IL-7, the high affinity of the IL-7Rα:IL-7 complex for γ_c further reduced the amount of free γ_c in a manner dependent on the concentration of IL-7. Measurements of bioluminescence resonance energy transfer (BRET) between IL-4Rα and γ_c were reduced when IL-7Rα was overexpressed. Furthermore, in a system expressing IL-7Rα, IL-4Rα, and γ_c, BRET between IL-4Rα and γ_c increased after IL-4 binding and decreased when cells were preexposed to IL-7, supporting the assumption that IL-7Rα and the IL-7Rα:IL-7 complex limit the accessibility of γ_c for other cytokine receptor complexes. We propose that in complex inflammatory environments, such asymmetric cross-talk establishes a hierarchy of cytokine responsiveness.

INTRODUCTION

Cytokines that belong to the common gamma chain family (referred to as γ_c cytokines) exert a broad spectrum of effects on lymphocytes, ranging from survival factor functions in resting naïve and memory T cell populations to differentiation-inducing functions in activated cells (*1*, *2*). Responses toward interleukin-2 (IL-2), IL-4, IL-7, IL-9, IL-21, and, to some degree, IL-15 (*3*) all require heterodimerization of the specific (also referred to as "private") cytokine receptor subunits with the "common" γ_c (*4*–*6*). This heterodimerization leads to the activation of the receptor-associated Janus kinase 1 (JAK1) and JAK3, which phosphorylate docking sites on the private receptor chains for signal transducer and activator of transcription (STAT) proteins (*7*). In addition to STAT activation, there are other unique signals encoded in the cytoplasmic tails of the private receptors chains, which, in part, explain the nonoverlapping biological effects of these cytokines.

The shared dependence of these cytokines on the γ_c for signaling raises the question of whether simultaneous or temporally proximal exposure to multiple γ_c cytokines could lead to a cross-talk between the signaling pathways that share γ_c. Whereas IL-7 plays a central role in survival of T cells, other γ_c cytokines also promote survival (*8*), T helper cell differentiation (*2*), antibody class switching (*9*), and the proliferation of T and B cells (*2*). Circulating naïve T cells can be exposed, during their scanning of antigen-presenting cells, to complex cytokine combinations in lymphoid environments. Cross-talk among γ_c cytokines has been reported at the transcriptional level at which long-lasting cytokine exposure can cross-regulate the amounts of private receptor chains (*10*–*13*). IL-7–mediated responses are inhibited in activated T cells due to passive sequestration of γ_c by a high abundance of IL-2 receptor α subunit (IL-2Rα) in those cells (*14*). However, this work did not investigate naïve cells and the possibility that cytokine stimulation modulates competition for γ_c. Modulation of competition mechanisms by cytokine-induced receptor chain interactions, as opposed to regulation of receptor abundances, has not been investigated beyond theoretical studies (*15*).

From a mechanistic point of view, such a cross-talk could result from limited numbers of γ_c, which may compromise cytokine-dependent complex formation of the γ_c with private receptor chains, a phenomenon described in other cytokine receptor systems, such as GM-CSF (granulocyte-macrophage colony-stimulating factor) and IL-3, which share the common β chain (*16*). This limited cytokine-dependent complex formation would depend on the concentrations of receptors on the cell surface and the affinity of the various private chains for the γ_c before and after cytokine binding. The affinity of the cytokine for its receptor is greater when γ_c is present, suggesting a higher stability of the trimeric complex of private chain, γ_c, and specific cytokine (*17*). Other studies found a substantial preassociation between unligated private chains and γ_c (*18*–*20*). These previous studies, however, did not address whether cytokine binding modulates the affinities between γ_c and private chains and whether simultaneous exposure of T cells to multiple common γ_c cytokines would lead to cross-talk among the pathways.

To address this gap in our understanding of γ_c cytokine signaling, we performed computational and quantitative experimental studies, relating receptor abundances and binding affinities to downstream signaling responses, and we found a fast-acting, highly sensitive, and

Computational Biology Unit, Laboratory of Systems Biology, National Institute of Allergy and Infectious Diseases, National Institutes of Health, Bethesda, MD 20892, USA.
*These authors contributed equally to this work.
†Present address: INSERM, U1043, Centre de Physiologie Toulouse-Purpan, Toulouse F-31300, France.
‡Present address: AstraZeneca, Respiratory, Inflammation and Autoimmunity iMed, Pepparedsleden 1, Mölndal, Sweden.
§Present address: Department of Chemical Engineering, Massachusetts Institute of Technology, Cambridge, MA 02142, USA.
¶Present address: Department of Anesthesia and Critical Care Medicine, Boston Children's Hospital, Harvard Medical School, Boston, MA 02115, USA.
‖Present address: University of Connecticut School of Medicine, Farmington, CT 06030, USA.
**Present address: Institut Necker Enfants Malades, INSERM U1151, CNRS, UMR8253, Faculté de Médecine, Université Paris Descartes, Sorbonne Paris Cité, Paris, France.
††These authors contributed equally to this work.
‡‡Corresponding author. Email: mms@niaid.nih.gov (M.M.-S.); rvarma@xencor.com (R.V.)
§§Present address: Xencor Inc., 111 West Lemon Avenue, Monrovia, CA 91016, USA.

asymmetrical cross-talk among the cellular responses toward stimulation with IL-4, IL-7, and IL-21. This response was caused by limiting numbers of γ_c. The results of detailed computational modeling of the cytokine signaling pathways combined with quantitative experiments ruled out several hypothetical mechanisms that were based on effects downstream of the receptor signal. Computational modeling supported by experiments that measure proximity among receptor chains [bioluminescence resonance energy transfer (BRET) measurements] suggested a cross-talk mechanism initiated by substantial preassociation between private receptor chains and γ_c and reinforced upon cytokine binding.

RESULTS

Sensitive and asymmetric cross-talk occurs among γ_c cytokine receptors

To investigate whether the shared dependence on the γ_c leads to cross-talk among γ_c cytokines, we focused on IL-4, IL-7, and IL-21 responses, because their receptors are present on naïve T cells and form heterotrimeric complexes consisting of the cytokine-bound private receptor chain and γ_c. On naïve T cells, these cytokines require γ_c for signal transduction (Fig. 1A). In other contexts, IL-4 signals through a complex consisting of IL-4Rα and IL-13Rα1. However, IL-13Rα1 protein is absent on the surface of naïve T cells (*21*). Cytokine binding leads to the phosphorylation of STAT transcription factors (Fig. 1A), which we assessed as readouts of pathway activation. Measuring the tyrosine phosphorylation of STAT1, STAT3, STAT5, and STAT6 in response to IL-4, IL-7, and IL-21, we found that STAT6 was exclusively phosphorylated in response to IL-4 stimulation (fig. S1A). IL-21 stimulation led to predominantly STAT3 phosphorylation (fig. S1B), in addition to STAT1 phosphorylation (fig. S1C). IL-7 stimulation almost exclusively induced phosphorylation of STAT5 (fig. S1D). To ensure that previous in vivo exposure to cytokines had not produced a high STAT tyrosine phosphorylation response that would have obscured the in vitro responses to cytokine exposure, we measured STAT tyrosine phosphorylation in naïve T cells without exogenous cytokine addition (fig. S1E). The extent of tyrosine phosphorylation of STATs in freshly isolated naïve T cells was low, and the cells responded uniformly (fig. S1E). This finding and the exclusive patterns of STAT tyrosine phosphorylation downstream of IL-4, IL-7, and IL-21 enabled the quantification of cross-talk among these three cytokines at the level of STAT phosphorylation.

To measure cross-talk, we performed sequential cytokine stimuli, each of 10-min duration. We chose 10 min because time-course measurements showed that STAT tyrosine phosphorylation in response to IL-4, IL-7, and IL-21 was saturated by that time (fig. S1, F to I). In experiments involving sequential cytokine stimuli, we found that IL-7 prestimulation led to a dose-dependent inhibition of STAT6 tyrosine phosphorylation by subsequent exposure to IL-4 (Fig. 1B). Low concentrations of IL-7 reduced the maximum of IL-4–dependent STAT6 phosphorylation without affecting the EC_{50} (dose at which 50% of the maximum response is achieved) of the response, whereas higher doses of IL-7 affected both the maximum response and the EC_{50} value (Fig. 1B). STAT molecules undergo phosphorylation at both tyrosine and serine residues as part of the cytokine-dependent activation process. IL-21 stimulated both STAT3 serine and tyrosine phosphorylation in a concentration-dependent manner (Fig. 1C and fig. S1B). We found that IL-7 prestimulation inhibited IL-21–dependent STAT3 serine and tyrosine phosphorylation to a similar extent (Fig. 1D). In this experiment, we used a concentration of IL-21 (50 pg/ml) that was similar to the EC_{50} of the IL-21 response (18 pg/ml; fig. S4C), because cytokine concentrations close to the EC_{50} are considered physiologically relevant (*22*, *23*). In contrast, prestimulation with neither IL-4 nor IL-21 affected the IL-7–induced tyrosine phosphorylation of STAT5 (Fig. 1, E and F), and IL-21 inhibited the IL-4–induced tyrosine phosphorylation of STAT6 (Fig. 1F). Together, these results indicate that IL-7 prestimulation inhibited the STAT phosphorylation (Fig. 1A) downstream of IL-4 and IL-21, but that neither IL-4 nor IL-21 inhibited IL-7 signaling to STATs. Thus, we found a fast (within 10 min) and asymmetric cross-talk among the IL-7, IL-4, and IL-21 signaling pathways.

Phosphorylated STAT (pSTAT) molecules can heterodimerize or homodimerize. If sequential IL-7 and IL-4 stimulation resulted in the formation of heterodimers of STAT5 and STAT6, this could have interfered with their recognition by the phosphorylation-specific antibodies, which could have confounded our interpretation of these experiments. We examined IL-7–dependent inhibition of IL-4 signaling in T cells derived from IL-7Rα-(Y449F) knock-in mice (*24*) and compared them with littermate wild-type controls. Tyr^{449} within the cytoplasmic tail of IL-7Rα serves as a docking site for STAT5 when phosphorylated; thus, as expected, IL-7–induced STAT5 phosphorylation was compromised in T cells from IL-7Rα–mutant (449F) mice (Fig. 1G). However, preexposure to IL-7 inhibited IL-4 responses in a concentration-dependent manner in T cells from either the IL-7Rα-(449F) mice or the littermate controls (Fig. 1H). In these experiments, we used a concentration of IL-4 (50 pg/ml) that was close to the EC_{50} value (85 pg/ml; fig. S4A). Thus, even in the absence of IL-7–induced STAT5 phosphorylation, which would prevent heterodimerization between STAT5 and STAT6 by subsequent IL-4 exposure, the presence of IL-7 inhibited IL-4 signaling. These results indicate that the effect of IL-7 on IL-4 responses is independent of the phosphorylation of Tyr^{449} in IL-7Rα, downstream signaling, and activation of STAT5, which would place the mechanism of inhibition before cytokine-induced receptor signal transduction.

Low numbers of γ_c relative to private cytokine-specific receptor chains lead to pathway cross-talk

To determine whether the cross-talk among γ_c cytokines resulted from limited availability of γ_c at the cell surface, we measured the numbers of γ_c molecules and the cytokine-specific private receptor chains present in peripheral naïve CD4 T cells from B10.BR mice. For these measurements, we used fluorescein isothiocyanate (FITC)–conjugated antibodies and analyzed the labeled cells by flow cytometry. We converted the fluorescence intensities of FITC to the number of FITC molecules using a standard curve generated with FITC beads with known numbers of FITC molecules. By measuring the dye to antibody ratio, we determined the number of antibodies bound for each receptor chain (see Materials and Methods). We found that γ_c was present at an average number of 550 molecules per cell and that the private receptor chains ranged from an average of 200 to 2000 molecules per cell (Fig. 2A). Thus, the sum of all the private chains present on these cells that signal through γ_c is about five times greater than the abundance of the shared component [mean, 5.4; 95% confidence interval (CI), 2 to 9.4].

γ_c cytokines provide survival signals at steady state to T cells and differentiation-inducing signals during T cell activation. To establish if γ_c numbers were limiting after T cell activation, we quantified γ_c family receptor numbers at various time points after T cell receptor (TCR) activation in vivo (fig. S2A) and in vitro (fig. S2B). The receptor numbers varied during the first few days after activation and then stabilized except for IL-7Rα, which increased without plateauing throughout

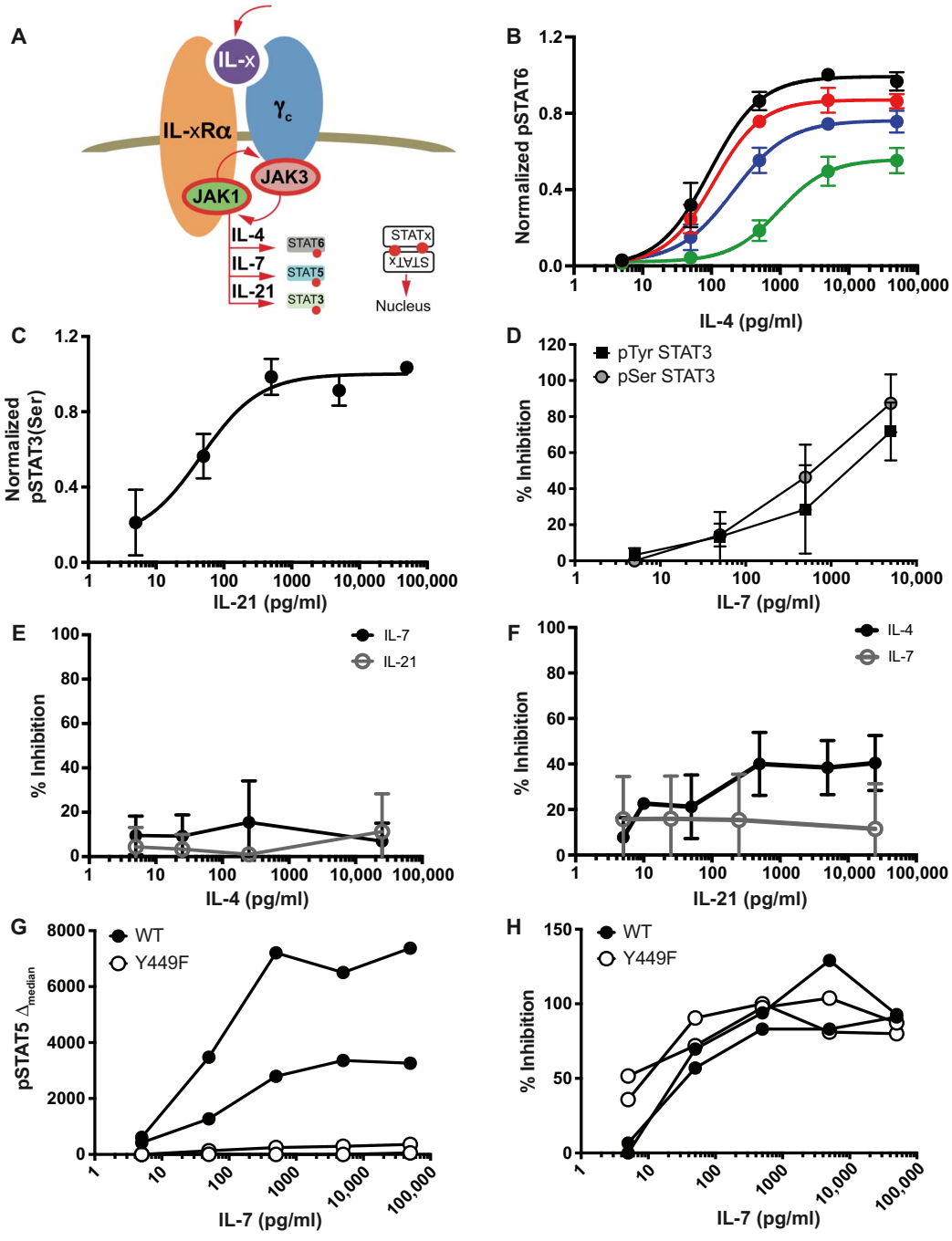

Fig. 1. Pretreatment of T cells with IL-7 suppresses subsequent responses to IL-4 and IL-21 in a dose-dependent manner. (**A**) Cytokine ligation and dimerization of the private receptor chains with the common γ_c lead to cross-activation of the associated Janus kinases JAK3 and JAK1. These kinases phosphorylate interaction sites on the receptors for STAT molecules that, in turn, are recruited and phosphorylated and then form STAT dimers that enter the cell nucleus to induce transcription. As discussed in the text, IL-4 specifically leads to activation of STAT6, IL-7 to activation of STAT5, and IL-21 to activation of STAT3. (**B**) Shifting IL-4 dose-response curves after pretreatment with varying doses of IL-7. Freshly isolated cells were stimulated for 10 min with increasing concentrations of IL-4 without IL-7 (black line) or pretreated with increasing concentrations of IL-7 (red, 50 pg/ml; blue, 200 pg/ml; green, 5000 pg/ml) for 10 min and stained with antibodies against pSTAT6. Maximum pSTAT6 response in the absence of IL-7 prestimulation was obtained from a fit for each experiment as described in Materials and Methods, and all pSTAT6 response values were normalized to it. (**C**) IL-21–induced STAT3 serine phosphorylation mimics STAT3 tyrosine phosphorylation. Freshly isolated cells were stimulated for 10 min with increasing concentrations of IL-21 and stained with antibodies directed against pSer^{727} in STAT3. Normalized pSTAT3 (Ser) values were obtained from a fit as in (B). (**D**) IL-7 pretreatment equally suppresses serine and tyrosine phosphorylations of STAT3. Freshly isolated cells were stimulated for 10 min with IL-21 (50 pg/ml) after pretreatment with increasing concentrations of IL-7 for 10 min. Percentage inhibition of IL-21–induced tyrosine or serine phosphorylation of STAT3 by IL-7 pretreatment was determined as described in Materials and Methods. Data presented in (B) to (D) were analyzed by flow cytometry by gating on CD4$^+$TCR$^+$CD44^{low} cells and are means ± SD from three independent experiments. (**E** and **F**) Asymmetry in cross-talk among γ_c cytokines. (E) Spleen and lymph node cells from B10.BR mice were stimulated for 10 min with IL-7 or IL-21 (50 pg/ml) without IL-4 or with increasing concentrations of IL-4 pretreatment for 10 min. Percentage inhibition of IL-7–dependent STAT5 phosphorylation or IL-21–dependent STAT3 phosphorylation was determined as described in Materials and Methods by gating on CD4$^+$TCR$^+$CD44^{low} cells. (F) Cells were stimulated for 10 min with IL-4 (50 pg/ml) or IL-7 (50 pg/ml) without IL-21 or with increasing concentrations of IL-21 pretreatment for 10 min. Percentage inhibition of IL-4–dependent STAT6 phosphorylation and IL-7–dependent STAT5 phosphorylation was determined as described in Materials and Methods by gating on CD4$^+$TCR$^+$CD44^{low} cells. Data in (E) and (F) are means ± SD of three independent experiments. (**G**) IL-7–induced STAT5 phosphorylation is lacking in IL-7Rα-449F-KI mice: IL-7–dependent STAT5 phosphorylation was measured by stimulating splenocytes from IL-7Rα-449F-KI mice (open circles) or wild-type (WT) littermate controls (filled circles) for 10 min. (**H**) IL-7–induced suppression of IL-4 responses is not affected in IL-7Rα-Y449F-KI mice. Splenocytes from IL-7Rα-Y449F-KI mice or WT littermate controls were stimulated for 10 min with increasing concentrations of IL-7 followed by stimulation with IL-4 (50 pg/ml). Percentage inhibition of IL-4–dependent STAT6 phosphorylation was determined as described in Materials and Methods. Data in (G) and (H) are individual measurements from two independent experiments (see also figs. S1, S2, and S4).

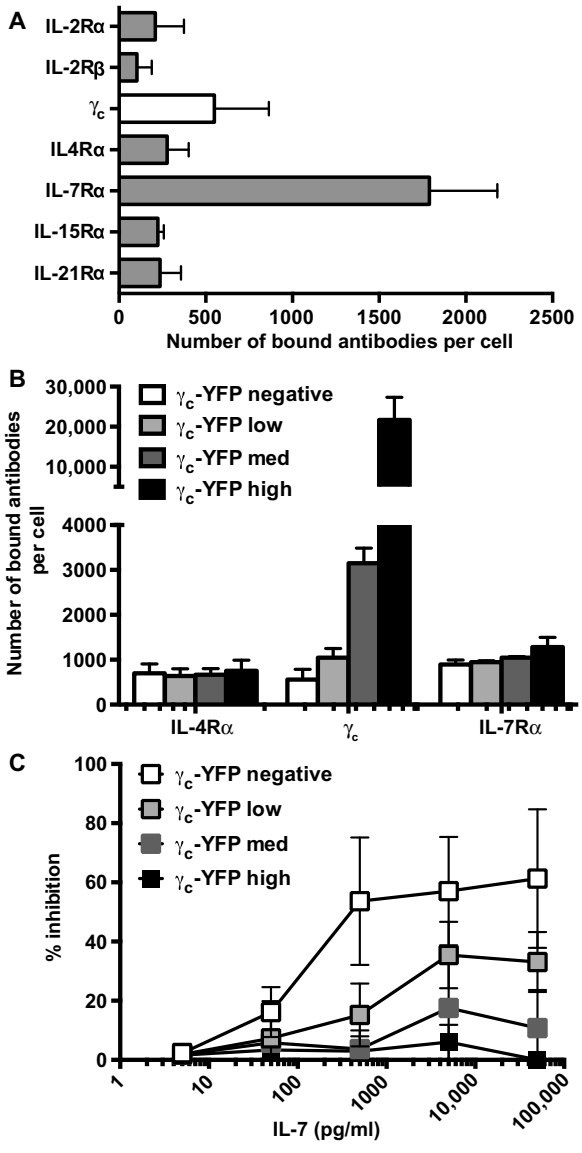

Fig. 2. Cytokine-specific private receptor chains outnumber the γ_c. (**A**) γ_c cytokine receptor chain abundance: Freshly isolated spleen and lymph node cells were stained with cytokine receptor antibodies, and the numbers of bound antibodies on $CD4^+TCR^+CD44^{low}$ cells were calculated as described in Materials and Methods. (**B**) γ_c-YFP abundance does not affect the abundance of IL-4Rα and IL-7Rα. Preactivated AND H^{2a*b} $CD4^+$ T cells were transfected with the pVenus–IL-2Rγ plasmid, after which the cell surface γ_c cytokine receptor numbers were determined as described in (A). (**C**) Overexpression of γ_c abrogates IL-7–induced suppression of IL-4 responses: The transfected cells in (B) were stimulated for 10 min with IL-4 (50 pg/ml) with or without pretreatment with increasing concentrations of IL-7 for 10 min. Percentage of inhibition of IL-4–induced STAT6 phosphorylation by IL-7 was determined after gating on cells expressing different amounts of γ_c-YFP (negative, low, med, and high). Data are means ± SD of at least three independent experiments (see also figs. S3 and S4).

the 30 days (fig. S2A). Despite variation in the private receptor chains, the ratio of γ_c to the private chains remained similar throughout the 30 days. We thus found that γ_c numbers are limiting when compared to the total number of private receptor chains both at steady state (Fig. 2A) and during T cell activation (fig. S2). To test the relevance of our findings for human immunology, we performed experiments on human $CD4^+$ T cells. As their murine counterparts, these cells had relatively low amounts of γ_c compared to the amounts of the private receptor chains (fig. S3A), and IL-4–dependent (fig. S3B) and IL-7–dependent (fig. S3C) STAT phosphorylation occurred at similarly low doses as for murine T cells. Asymmetric cross-talk was also observed in human cells where IL-7–mediated inhibition of subsequent IL-4 responses occurred, but not the reverse (fig. S3D), suggesting that these features of the γ_c cytokine signaling pathway are conserved between mice and humans.

To directly test whether the observed cross-talk was due to the limiting numbers of γ_c, we modulated the cell surface concentration of γ_c by transfecting preactivated primary $CD4^+$ T cells from B10.A-AND mice with a γ_c-YFP (yellow fluorescent protein) construct and measured cross-talk in cells expressing different amounts of γ_c. We observed that the abundance of γ_c in γ_c-YFP negative cells was similar to that of untransfected cells. The fold increase relative to γ_c-YFP negative cells for γ_c-YFP low was 2 ± 0.5, γ_c-YFP med was 6 ± 2, and γ_c-YFP high was 32 ± 17, without altering the amount of IL-4Rα or IL-7Rα (Fig. 2B). Increasing γ_c numbers at the cell surface reduced the inhibition of IL-4 responses by IL-7 pretreatment and even abolished it at high γ_c abundance (Fig. 2C). In addition, IL-4 and IL-7 pathways showed greater STAT phosphorylation in cells with higher amounts of γ_c except in γ_c-YFP high cells (fig. S3, E and F). These data are consistent with the hypothesis that IL-7–dependent inhibition of IL-4 signaling results from limiting numbers of γ_c.

STAT phosphorylation and cross-talk require low percentages of cytokine-bound surface receptors

One possible interpretation of the dependence of the suppressive cross-talk on the cell surface concentration of γ_c and IL-7 is that IL-7Rα ligation sequesters a substantial fraction of γ_c. The extent of suppression induced by sequestration of γ_c by ligated IL-7Rα would depend on how many IL-4:IL-4Rα:γ_c or IL-21:IL-21Rα:γ_c trimeric receptor complexes are needed for efficient signaling. We therefore measured the dose-response characteristics of STAT phosphorylation for IL-4, IL-7, and IL-21 and found that they exhibited sigmoidal dose-response curves, with EC_{50} values ranging from 10 to 100 pg/ml (fig. S4, A to C). On the basis of previously published affinity measurements (*25*–*27*) and our own measurements (table S1; fig. S4, D to G; and Materials and Methods) of the K_d (dissociation constant) values of IL-4, IL-7, and IL-21 for their respective private receptor chains, we converted cytokine concentrations into numbers of cytokine-bound receptors. At EC_{50} concentrations, the number of cytokine-bound receptors varied between 2 and 13 for both IL-4 (Fig. 3A) and IL-21 (Fig. 3B) and between 1 and 70 for IL-7 (Fig. 3C). These receptor occupancies represent the upper bound on the number of trimeric complexes required for half-maximal STAT responses.

Using this methodology, we estimated the average number of γ_c molecules recruited to IL-7–bound IL-7Rα chains at IL-7 concentrations for which we observed cross-talk. By plotting the IL-7–dependent suppression of IL-4–induced STAT6 phosphorylation (Fig. 3D) and IL-21–induced STAT3 phosphorylation (Fig. 3E) as a function of IL-7R occupancy, we determined that a small number of occupied IL-7R inhibited IL-4 and IL-21 responses. IL-7 (50 pg/ml; a concentration within the EC_{50} range for IL-7) that bound between 4 and 40 IL-7Rα chains (depending on the assumed K_d for the IL-7Rα:γ_c interaction) led to an average of 35% inhibition of the response to subsequent exposure to IL-4 (50 pg/ml; a concentration close to its EC_{50} of 85 pg/ml) (Fig. 3D). Thus, IL-4 and IL-21 responses were inhibited in a highly sensitive

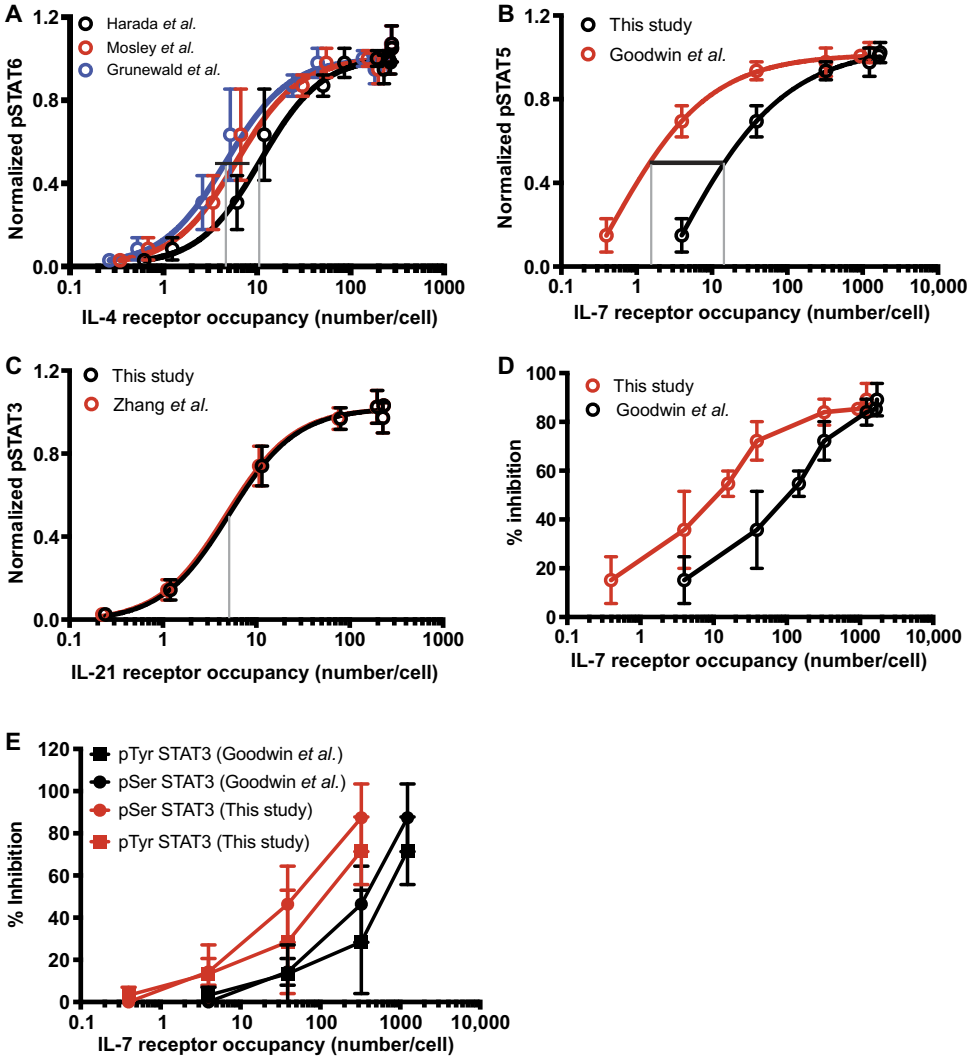

Fig. 3. Low receptor occupancy is sufficient for STAT phosphorylation and suppressive cross-talk. (**A** to **C**) IL-4, IL-7, and IL-21 responses are highly sensitive. Freshly isolated T cells were stimulated for 10 min with increasing concentrations of IL-4 (A), IL-7 (B), and IL-21 (C); stained with antibodies against pSTAT molecules; and analyzed by flow cytometry by gating on $CD4^+TCR^+CD44^{low}$ cells. Normalized STAT phosphorylation values were determined as described in Materials and Methods and plotted against receptor occupancy. Doses of cytokines were converted into receptor occupancies using K_d values obtained experimentally (fig. S5) or from the literature (table S1) and the receptor numbers obtained in Fig. 2A. Data are means ± SD of 11 to 20 independent experiments. (**D** and **E**) Few ligated IL-7Rs suffice to suppress IL-4 and IL-21 responses. T cells were stimulated for 10 min with IL-4 (50 pg/ml) (D) or IL-21 (50 pg/ml) (E) with increasing concentrations of IL-7 prestimulation. Percentage inhibition of IL-4 (D) or IL-21 (E) response by IL-7 pretreatment was determined as described in Materials and Methods and plotted against IL-7R occupancy obtained as described in (B). Data are means ± SD of 4 to 13 independent experiments (see also fig. S4 and table S1).

manner by pretreatment with IL-7, which occurred under conditions in which each cytokine signal led to only small numbers of active trimeric receptor complexes (private chain, γ_c, and cytokine). These results suggest that recruitment of γ_c to ligated receptors could not be the sole cause of cross-talk.

Another parameter that can control the cell surface abundance of molecules is endocytosis and intracellular trafficking. γ_c and many other cytokine receptors undergo constitutive and ligand-induced endocytosis (*28*). IL-4 signaling through type 1 and type 2 receptors might exclusively occur from within endocytic compartment (*29*, *30*). Therefore, an alternative hypothesis explaining the observed IL-7–dependent cross-talk is that IL-7 binding leads to endocytosis such that the amount of γ_c at the cell surface becomes limiting for signaling by cytokines that the cell encounters after encountering IL-7. We tested this hypothesis by measuring the abundance of γ_c on the surface of T cells from human peripheral blood mononuclear cells (PBMCs) after exposure to low and high concentrations of IL-4 and IL-7. We found no major change in the cell surface abundance of γ_c during the time frame of cytokine exposure to cells, suggesting that, in our experimental system, internalized γ_c might be recycled to the cell surface, leading to a steady state in the availability of γ_c at the cell surface (fig. S5).

Computational modeling identifies potential mechanisms of pathway cross-talk

The high sensitivity of the IL-4 system to prestimulation of the cells with IL-7 represented a quantitative riddle: If the IL-4 receptor needs to recruit only few γ_c molecules for a half-maximal response, then how can an IL-7 dose that recruits only a small fraction of the γ_c molecules to IL-7Rα reduce IL-4–induced STAT6 phosphorylation so substantially? The affinity of γ_c for the private receptor chains before cytokine binding determines the fraction of γ_c that is associated with each private chain at steady state. Upon cytokine binding, however, this affinity may change in a manner analogous to the way in which γ_c increases the affinity of the cytokine-receptor interaction (*31*). Thus, even a simple representation of the signaling components leading to STAT phosphorylation encompasses multiple independent parameters that might affect the signal output, rendering a purely intuitive understanding of the observed cross-talk difficult. We therefore built a computational model of the involved signaling pathways using the modeling software Simmune (Supplementary Modeling File, section 1) (*32*–*34*). We used Simmune because this program enables a visual representation for defining molecules and their interactions and provides tools for exploring the behavior of computational models (Supplementary Modeling File, section 2). Using the model input, Simmune generates coupled ordinary or partial differential equations (ODEs or PDEs) and solves these equations numerically. Because in our model we assumed that the responding cells could be represented as simple entities without specific spatial features beyond the presence of a membrane-bounded cytoplasm, Simmune generated only ODEs to represent our model. We used Simmune to calculate the changes in the concentrations

of the involved signaling components over time and perform a quantitative comparison between model behavior and the experimental data. We used the Simmune Analyzer to explore unknown parameters over their physiologically reasonable ranges and determine their effect on model behavior (Supplementary Modeling File, section 3), represented as STAT phosphorylation in our model. Using this approach, we explored which combinations of parameters would enable the model to align with the experimental data and whether the relationships among parameters could be further explored experimentally (Supplementary Modeling File, section 4).

A computational model illustrates how sequestration by IL-7Rα results in limited availability of γ_c for IL-4 signaling and asymmetric cross-talk

We constructed a computational model that consisted of basic elements of the cytokine signaling pathways: the receptor chains (IL-4Rα, IL-7Rα, and γ_c), receptor-associated JAKs, and the cytokine-specific STATs. We also included constitutively active phosphatases that reversed the phosphorylation of docking sites on receptor chains and STATs. To account for our limited knowledge of the molecular interaction parameters, our simulations sampled these parameters over a wide range of physiologically reasonable values (table S2). Association rates were varied between 10^4 (10^3 for interactions within the cell membrane) and 5×10^7 (in membrane, 10^6) liter/(mol s). Dissociation rates were varied between 0.01 and 10 per second, whereas transformation rates (for example, between phosphorylated and unphosphorylated states) were varied between 0.0001 and 1 per second. Cytosolic protein concentrations were varied between 0.1 and 500 nM. Affinities of the private receptor chains for the γ_c before and after ligand binding were varied. We then compared the simulated STAT phosphorylation profile resulting from the exposure to a specified concentration of a single cytokine and IL-7–dependent inhibition of IL-4 signaling to their experimental counterparts (fig. S6, A to C). The model achieves phosphorylation of a physiologically relevant fraction of the total pool of available STAT molecules (fig. S6, D and E) in response to IL-4 and IL-7 stimulation. Thus, the experimental data acted as constraints on the parameter values, enabling the identification of several parameter combinations that reproduced those data. These constraints were sufficient to rule out many regions in parameter space. The remaining valid parameter combinations shared two critical features: a higher affinity of γ_c for unligated IL-7Rα than for the unligated IL-4Rα and a higher affinity of γ_c for the ligated private chains over the unligated ones (Fig. 4A). With these identified parameter combinations, we tested the consistency of the model's behavior and performed simulations with increasing concentrations of γ_c without changing the other parameters. In agreement with our experimental findings, these simulations showed greatly reduced inhibition (fig. S6, F and G). Furthermore, reversing the order of cytokine stimuli led to only very modest inhibition (fig. S6H), consistent with the asymmetry of inhibition observed experimentally (Fig. 1, E and F).

Our modeling results are consistent with the following mechanism contributing to asymmetric suppressive cross-talk: The substantial basal affinity of γ_c for the unligated IL-7Rα chain that is expressed in large amounts on the cell surface leads to sequestration of a major fraction of γ_c before cytokine stimulation occurs (Fig. 4B). The increased affinity of γ_c for the ligated IL-7R enables even low concentrations of IL-7 to generate ligated IL-7Rα chains that capture a sufficiently large number of the remaining free γ_c (Fig. 4C) to limit its availability such that IL-4 signals became suppressed through limited IL-4:IL-4Rα:γ_c complex formation (Fig. 4D). Private receptor chains for IL-4 and IL-21 are present at concentrations lower than that of IL-7Rα and, upon ligation, do not have enough affinity for γ_c to sequester it away from IL-7Rα, which results in asymmetric cross-talk.

Another potential explanation for the ability of low IL-7 concentrations to suppress IL-4 signaling involves IL-7–induced dephosphorylation of key signaling components, in particular of the docking sites on cytokine receptor chains or the STAT proteins. We considered this mechanism of asymmetric suppressive cross-talk because phosphatases have been reported to control cytokine receptor signaling (*35*, *36*) and JAK-mediated STAT phosphorylation (*37*). Simulations helped us to determine relationships among parameters for these phosphatase models that we could test experimentally. The results of these experiments suggested that such induced phosphatase-based models were not plausible (Supplementary Modeling File, section 3 and fig. S7).

IL-7Rα competes with IL-4Rα to form complexes with γ_c

Our modeling results predicted that IL-7Rα sequesters free γ_c. We thus tested whether the IL-7–induced inhibition of IL-4 signaling depended on the abundance of IL-7Rα in naïve T cells. To study the effect of IL-7Rα abundance, we used T cells from three populations of mice: "AND TCR transgenic (H^{2b})" mice, the B10.Br (H^{2k}) mice, and B10.A-AND (H^{2a*b}) mice. T cells from the B10.A (H^{2a}) mice had the highest amounts of IL-7Rα and γ_c, those from the AND TCR transgenic (H^{2b}) mice had the lowest amounts of IL-7Rα and less γ_c, and those from the B10.A-AND (H^{2a*b}) mice had an intermediate amount of IL-7Rα at the cell surface with a similar amount of γ_c to that of the cells from the AND TCR transgenic (H^{2b}) mice (Fig. 5A). By analyzing the responses of T cells from these strains of mice, we found that IL-7–induced inhibition of IL-4 signaling correlated positively with IL-7Rα abundance (Fig. 5B).

We tested whether both the unbound and IL-7–bound IL-7Rα chains competed with IL-4Rα for the recruitment of γ_c with a BRET assay that monitored the interaction between γ_c fused to luciferase (donor) and IL-4Rα fused to the YFP variant Venus (acceptor). Modulation of the association between IL-4Rα and γ_c by varying the cell surface abundance of IL-7Rα and IL-7 stimulation would produce changes in the BRET signal. To avoid the presence of untagged endogenous receptor chains on the cell surface, we expressed IL-7Rα, IL-4Rα–YFP, and γ_c-luciferase chains in Chinese hamster ovary (CHO) cells, which lack these receptors, using plasmids in the following proportion: IL-7Rα to IL-4Rα–YFP to γ_c-Rluc (4:1:1). When the cells were treated with IL-4, the BRET signal increased. Pretreatment with either a high or low concentration of IL-7 reduced the IL-4–induced BRET signal (Fig. 5C). The association between IL-4Rα and γ_c in the absence of any added cytokine was greater when IL-7Rα was replaced by the interferon-γ (IFN-γ) receptor 2 (IFNGR2) (Fig. 5D). These data are consistent with the model suggesting that engaged and unengaged IL-7Rα chains can reduce the number of IL-4Rα:γ_c complexes formed at the cell surface.

DISCUSSION

Here, we systematically investigated how the low abundance of γ_c relative to that of the cytokine private chains that require it for signaling could lead to cross-talk among those receptors. We observed a fast-acting and asymmetric cross-talk wherein IL-7 inhibited IL-4– and IL-21–induced responses in naïve CD4 T cells, but not vice versa. Previous work established the existence of a cross-talk among γ_c cytokines at the transcriptional level (*10*, *12*, *13*, *38*, *39*); however, the cross-talk we

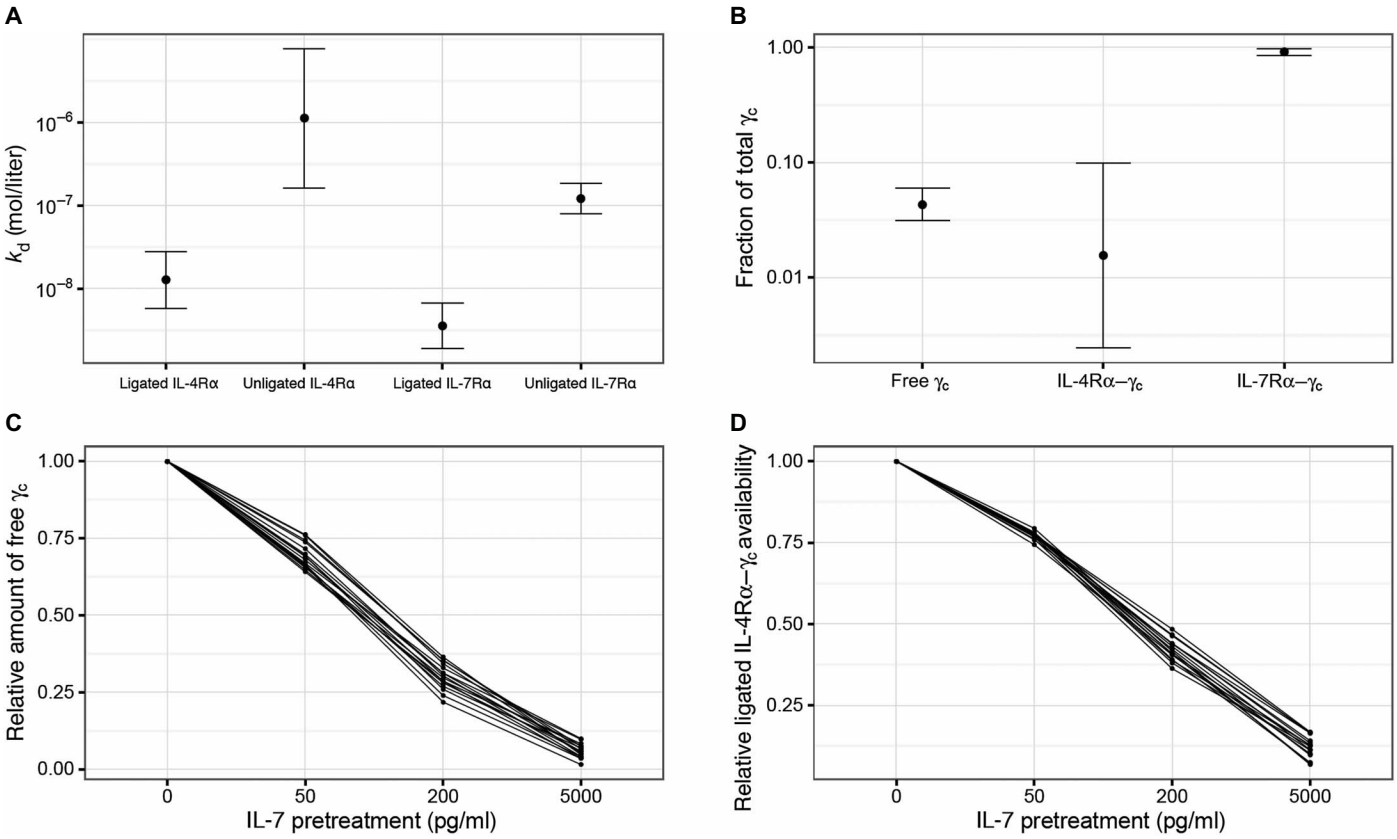

Fig. 4. Computational model explaining suppressive cross-talk originating at the receptor level. (**A** and **B**) Preassociation with IL-7Rα limits the availability of γ_c for signaling through IL-4Rα. (A) Computationally predicted affinities (K_d) of the γ_c for the private receptor chains with and without cytokine ligation. (B) Distribution of γ_c between unbound, IL-4Rα–bound, and IL-7Rα–bound states before cytokine stimulation. Data are means ± SD from 16 simulations using parameter sets matching the experimental constraints in table M1 (Supplementary Modeling File). (**C** and **D**) The limited number of γ_c results in fewer IL-4–ligated IL-4Rα–γ_c complexes that can induce STAT6 phosphorylation. (C) Fraction of free γ_c relative to unstimulated cells [corresponding to the left point in (B)] for increasing doses of IL-7 10 min after stimulation. (D) Pretreatment with increasing doses of IL-7 leads to increasingly reduced input signal for STAT6 phosphorylation. The graph shows the fraction of IL-4–ligated IL-4Rα–γ_c complexes relative to cells without IL-7 pretreatment. The plotted lines in (C) and (D) represent results from simulations using 16 parameter sets matching the experimental constraints in table M1 (Supplementary Modeling File; see also fig. S6).

describe here is distinct from that previously reported because it occurs at the level of receptors without changes in their concentration and acts on much shorter time scales. Computational models of γ_c cytokine signaling that were generated with Simmune and the Simmune Analyzer enabled us to propose a mechanism that explains the suppressive cross-talk. The features of this mechanism include a combination of (i) the high affinity of the unligated IL-7Rα chain for γ_c, resulting in "preassociation" of the receptor chains, and (ii) a strong increase in affinity between these two chains when IL-7Rα binds to IL-7, demonstrating "affinity conversion" after cytokine stimulation. Several lines of experimentation confirmed such an affinity-driven mechanism of cross-talk. In particular, cross-talk was found to be sensitive to the amount of γ_c and correlated with IL-7Rα abundance.

Note that the computational models we used to test our biological hypotheses quantitatively, through simulations, contain only signaling components and mechanisms that are directly accessible experimentally. The signaling molecules interact through binding sites that have been identified previously and with mass action kinetics based on the abundances of (multi-)molecular complexes and first- or second-order reaction rates. This has several advantages. First, it makes the modeling process accessible to investigators who would not consider themselves "modelers." There are no assumptions hidden in phenomenological mathematical functions shaping the model's behavior. Second, experimental manipulations (for example, mutations of specific binding sites) are reproduced naturally in the model. Third, parameter ranges have natural biophysically plausible bounds because we know, for example, what association rates are possible between membrane-bound and cytosolic signaling components. This constrains our parameter searches in a natural way. Fourth, the range of dose-response characteristics and signaling dynamics is limited by what can be generated through first-order (transformations and dissociations) and second-order (associations) molecular reactions. The latter two points, concerning parameter ranges and possible kinetics, are particularly important for our approach (using the Simmune Analyzer) aiming at exhaustively analyzing the possible characteristics of competing models. Without those constraints, excluding models based on parameter screens would be far more difficult. Fortunately, the present signaling networks downstream of the γ_c-dependent cytokine receptors are sufficiently simple to permit the use of our strategy. Other systems may be far more complicated or less well explored and may require more phenomenological modeling approaches because the detailed approach used here would introduce too many ad hoc mechanistic assumptions or would simply become overwhelmingly complex.

Basal affinities between γ_c and private chains have been assumed or reported by others (*18*, *19*, *40*), but our data illustrate the importance of

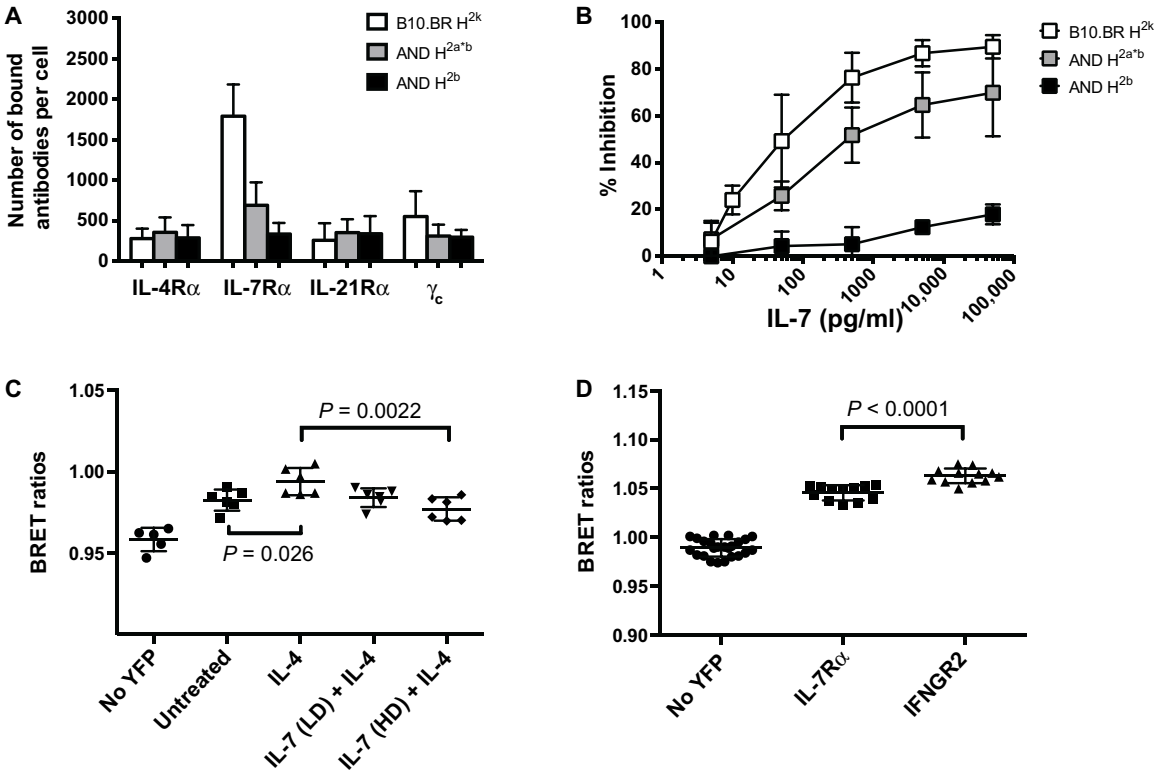

Fig. 5. Suppressive cross-talk correlates with IL-7Rα abundance, and engaged IL-7Rα reduces the ability of IL-4Rα to form complexes with γ_c. (**A**) The cell surface γ_c cytokine receptor numbers were determined as in Fig. 2A for freshly isolated cells from B10.BR, AND X B10.A (F1-AND H^{2a*b}), and AND H^{2b} mice by gating on $CD4^+TCR^+CD44^{low}$ cells. (**B**) Freshly isolated cells from B10.BR (B10.BR H^{2k}), AND X B10.A (F1-AND H^{2a*b}), and AND (H^{2b}) mice were stimulated as described in Fig. 3D, and the percentage inhibition of IL-4 signaling by pretreatment with IL-7 in $CD4^+TCR^+CD44^{low}$ cells was determined. Data are means ± SD of three independent experiments. (**C**) BRET assays were performed in CHO cells after cotransfection with phRluc–IL-2Rγ (donor), pVenus–IL-4Rα (acceptor), and pcDNA3.1–IL-7Rα (see Materials and Methods). BRET between γ_c and IL-4Rα is expressed as the ratio between the fluorescence of the acceptor (YFP) over the luciferase activity of the donor. BRET ratios from cells not expressing YFP are also shown as a baseline. Cells were stimulated with IL-4 (50,000 pg/ml) for 10 min with or without IL-7 pretreatment with IL-7 {100 pg/ml [low dose (LD)] or 5000 pg/ml [high dose (HD)]} for 10 min. (**D**) Replacing IL-7Rα with the IFN-γ receptor increases BRET between IL-4Rα and γ_c. Data are means ± SD of 5 to 12 replicates from one of two independent experiments. Mann-Whitney tests were performed to determine statistical significance.

the differences in affinities between the chains in determining the basal pools of preformed complexes of private cytokine receptor chains and γ_c. Our modeling results led us to postulate a hierarchy of affinities between engaged and unengaged IL-7Rα and IL-4Rα for γ_c. Within this hierarchy, the ligated IL-7R has the highest affinity for γ_c, which is followed by the ligated IL-4R. Among the nonligated private chains, IL-7Rα can outcompete IL-4Rα for γ_c. The BRET assays confirmed a substantial basal association of the private IL-7R chain with γ_c because expression of the former reduced the formation of IL-4Rα:γ_c complexes. In addition, consistent with our conclusions, several groups have reported a low affinity of unbound IL-4Rα for γ_c (*41*, *42*). In addition to the affinity of the unligated IL-7Rα chain for the γ_c, a critically important feature of the proposed model was the strong increase in affinity between these two chains when IL-7Rα was bound by IL-7. The first suggestion of a cytokine ligation–induced increase in the affinity between private cytokine chains and γ_c came from Saito and colleagues (*17*). The combination of experimental data and computational simulations reported here corroborates the cytokine-driven affinity conversion model proposed by Kondo and colleagues (*31*) and extends it to other members of the IL-2R family, in particular IL-7R.

γ_c cytokines other than IL-7, including IL-4, are also known to promote cell survival and the regulation of naïve cell homeostasis (*8*). In light of our findings, we suggest a reevaluation of a long-standing hypothesis about the functional relevance of IL-7Rα down-regulation in activated cells. It is generally thought that IL-7 is a limiting cytokine, and down-regulation of IL-7Rα on activated T cells has been assumed to represent an altruistic response, reducing the amount of IL-7 taken up by strongly proliferating clones (*13*). An alternative explanation is that this response may enable T cells to use IL-4 signals for survival and differentiation. In addition, in support of this interpretation, changes in the abundances of the private chains for IL-2, IL-4, and IL-15 after T cell activation inversely mirror those of IL-7 and IL-21, the two dominant cytokines capable of inhibiting the responses toward IL-4 (fig. S3). The cross-inhibition phenomenon may thus enable the cells to prioritize cytokine signals for survival in vivo, where the availability of these cytokines is scarce.

Finally, our work also sheds light on the importance of regulating cytokine receptor abundance in X-linked severe combined immunodeficiency (X-SCID) patients receiving autologous stem cell transplants reconstituted with γ_c. Human subjects deficient in the expression of γ_c or JAK3 suffer from X-SCID, which is characterized by a loss of T and natural killer (NK) cells and the presence of nonfunctional B cells (*5*). A promising therapy for such patients is the transplantation of autologous stem cells that have been reconstituted with γ_c (*43*, *44*). In gene therapy

trials, although many patients have benefited from this approach, some of them develop lymphoproliferative disorders (*45*, *46*), which are in part correlated with the extent of γ_c reconstitution (*47*, *48*). The importance of strictly controlled γ_c amounts was further emphasized in studies in which the low abundance of γ_c led to the development of T cells but not NK cells, whereas intermediate amounts of reconstituted γ_c supported the development of both T cells and NK cells, but with the NK cells exhibiting poor survival (*49*). Moreover, as our results suggest, it may not only be sufficient to carefully restore the abundance of γ_c but also be important to monitor IL-7Rα abundance to maintain appropriate cytokine responses in naïve cells in vivo.

MATERIALS AND METHODS

Reagents and antibodies

FITC-conjugated anti-mouse IL-2Rβ (clone TM-Beta1), anti-mouse IL-2Rγ (clone 4G3), unconjugated or phycoerythrin (PE)–conjugated anti-mouse IL-4Rα (clone mIL-4Rα–M1), PE-Cy7–conjugated anti-mouse IL-7Rα (clone SB/199), Pacific blue–conjugated anti-mouse CD4 (clone RM4-5), and PE-Cy7–conjugated anti-mouse CD44 (clone IM7) antibodies were purchased from BD Biosciences. Alexa Fluor 647–conjugated anti-mouse IL-7Rα (clone A7R34) and anti-mouse IL-21Rα (clone 4A9) antibodies were purchased from BioLegend. FITC-conjugated anti-mouse IL-7Rα (clone A7R34) antibody was purchased from eBioscience, and anti-mouse IL-15Rα antibody was purchased from R&D Systems. Alexa Fluor 488–conjugated anti-mouse TCR β-chain (clone H57) antibody was purchased from Invitrogen. Anti-mouse IL-2Rγ antibody (clone TUGm3) was a gift from I. Naoto (Tohoku University), and anti-mouse IL-2Rα antibody (clone PC61) was a gift from N. Singh (University of Maryland, School of Medicine). Anti-CD16/CD32 antibody (clone 2.4G2) was obtained from Biovest International Inc. and was used to block Fc receptors. Alexa Fluor 647–conjugated anti–phospho-STAT3 (pY705), anti–phospho-STAT3 (pS727), anti–phospho-STAT5A (pY694), and anti–phospho-STAT6 (pY641) antibodies were also purchased from BD Biosciences. All the cytokines were purchased from PeproTech Inc. JAK3 inhibitor (CP-690550) was purchased from Selleck Chemicals.

Cytokine receptor constructs

The plasmid pMIG–IL-7Rα–IRES–GFP was a gift from S. Durum and was used as a source of IL-7Rα complementary DNA (cDNA). The IL-7Rα open reading frame (ORF) was transferred into the plasmid pcDNA3.1(+)MycHis A between Nde I and Xho I to generate pcDNA3.1–IL-7Rα. The plasmid pVenus–IL-2Rγ was generated by inserting the mouse IL-2Rγ ORF (Open Biosystems) into the plasmid pVenus N1 (Clontech) between the Xho I and Xma I sites. The plasmid phRluc–IL-2Rγ was generated by inserting the IL-2Rγ ORF (Open Biosystems) into the plasmid phRluc N1 (PerkinElmer) between the Xho I and Bam HI sites. The plasmid pVenus–IL-4Rα was generated by inserting the IL-4Rα ORF (Open Biosystems) into the plasmid pVenus N1 (Clontech) between the Xho I and Xma I sites.

Cells and mice

All strains of mice used in this study were obtained from the National Institute of Allergy and Infectious Diseases (NIAID) contract facility (Taconic Farms). The IE^k-restricted moth cytochrome C (MCC)–specific TCR transgenic AND mice (H^{2b}) on a $Rag2^{-/-}$ background were crossed to B10.A, $Rag2^{-/-}$ (H^{2a}) mice to generate B10.A.AND mice (H^{2a*b}) on a $Rag2^{-/-}$ background. Unless otherwise specified, the naïve T cells used in this study were isolated from B10.BR mice. All animals used in this study were maintained in a specific pathogen–free environment, and the NIAID Animal Care and Use Committee approved all experiments. Cells were isolated from pooled lymph nodes and spleen. When needed, isolated cells from B10.A.AND or AND mice were activated with 10 μM MCC and splenocytes from B10.A, $CD3\varepsilon^{-/-}$ mice in Advanced Dulbecco's modified Eagle's medium supplemented with 2.5% fetal bovine serum, as described previously (*50*). Exogenous IL-2 was added (50 U/ml) every 2 days until day 6 of activation when the cells were used. Transfections of activated cells were performed with Amaxa Technology according to manufacturer's instructions and as described previously (*51*). Splenocytes from IL-7Rα-(Y449F) knock-in mice and their littermates were a gift from N. Abraham. Frozen human PBMCs from human blood samples were obtained from J. Milner.

Receptor quantification by flow cytometry

We obtained commercial antibodies free of carrier proteins and conjugated them with either FITC or Alexa Fluor 647 according to the manufacturer's instructions. After labeling, the dye to protein ratio for each labeling reaction was determined. Freshly isolated cells were stained in fluorescence-activated cell sorting (FACS) buffer [phosphate-buffered saline (PBS), 1% bovine serum albumin (BSA), and 0.02% sodium azide] with cytokine receptor–specific antibodies at saturating concentration at 4°C after Fc receptors were blocked. Naïve CD4 T cells were analyzed by gating on $CD4^+$, TCR^+, and $CD44^{low}$ cells. A calibration curve correlating the fluorescence measured by flow cytometry to the number of Alexa Fluor 647 or FITC molecules was established with Quantum FITC-5 or Quantum Alexa Fluor 647 molecules of equivalent soluble fluorochrome calibration beads (Bang Laboratories). Median fluorescence intensity (MFI) was calculated by subtracting the median fluorescence of the isotype control for each cytokine receptor antibody staining. The calibration curve was used to calculate the number of equivalent soluble fluorochromes corresponding to each corrected MFI. Using the dye:protein ratio measured earlier, the average number of bound antibodies per cell was calculated. These measurements and calculations were repeated five times (three times for IL-2Rα/β) (table S3). To obtain CIs for the ratio of γ_c numbers to the sum of the receptor chains interacting with it, we generated 1000 permutated samples of receptor number combinations (for each receptor randomly selecting from the measurements) and calculated the resulting ratio #(γ_c):#(all dependent receptor chains). These ratios were sorted so that the 50th value would give the lower limit and the 950th value would give the upper limit of the 95% CI.

Analysis of pSTAT by flow cytometry

Freshly isolated cells were stimulated with varying concentrations of cytokines in Hepes-buffered saline [20 mM Hepes (pH 7.5), 137 mM NaCl, 5 mM KCl, 0.7 mM Na_2HPO_4, 6 mM D-glucose, 2 mM $MgCl_2$, and 1 mM $CaCl_2$] supplemented with 0.5% BSA at 37°C. To stop the stimulation, tubes were immediately transferred to ice and fixed with 4% paraformaldehyde for 2 min. After extensive washing with PBS–0.5% BSA, the cells were fixed in 90% methanol for 15 min at −20°C. After washing and blocking Fc receptors, the cells were stained in FACS buffer to detect pSTAT proteins and cell surface markers. The STAT phosphorylation status of naïve CD4 T cells was determined by flow cytometry after gating on $CD4^+TCR^+CD44^{low}$ cells. For dose responses, the MFI of untreated cells was subtracted from the MFI of each sample to obtain Δ_{median} values. These pSTAT Δ_{median} values were plotted

against cytokine concentration to obtain dose-response curves, which were subsequently fitted using the log(agonist) versus response-variable slope equation

$$Y = \text{Bottom} + \frac{(\text{Top} - \text{Bottom})}{(1 + 10^{((\text{LogEC}_{50} - X)*\text{HillSlope})})}$$

in GraphPad Prism software (www.graphpad.com/guides/prism/6/curve-fitting/index.htm?reg_dr_stim_variable.htm). The data were then normalized to the saturated response as determined by the fit. A global fit was performed on the normalized data to obtain the EC_{50} concentration of cytokine at which a half-maximum response was generated. For inhibition experiments, the first cytokine was added for 10 min and then, without washing, the second cytokine was added to the sample for another 10 min. The same protocol was used for fixation, staining, fluorescence measurement, and Δ_{median} calculation. To assess to what extent the preincubation affected the signaling of the second cytokine, the percentage inhibition was calculated as

$$\%\text{Inhibition} = 100 - \left\{\frac{\Delta_{median}\text{pSTAT(dual cytokine treated cells)}}{\Delta_{median}\text{pSTAT(second cytokine treated cells)}}\right\}*100$$

Receptor occupancy calculation

Fractional receptor occupancy was calculated as

$$\%R_{occupancy} = \frac{[\text{cytokine}]}{([\text{cytokine}] + K_d)} * 100$$

The K_d values for each cytokine were obtained from literature or calculated with our own assay (see fig. S4). The numbers of receptors occupied at each concentration were then calculated using the total number of receptors obtained from Fig. 2.

Bioluminescence resonance energy transfer

The cDNA of *Renilla* luciferase was fused to the C terminus of IL-2Rγ cDNA (phRluc–IL-2Rγ) and used as a donor of energy, whereas the C terminus of IL-4Rα cDNA was fused to a variant of YFP (Venus) (pVenus–IL-4Rα) and used as an acceptor. CHO cells were cotransfected with phRluc–IL-2Rγ, pVenus–IL-4Rα, and pcDNA3.1–IL-7Rα in the proportion 1:1:4 with X-tremeGENE HP DNA Transfection Reagent (Roche Applied Science) at a ratio of 3 μl of reagent per microgram of DNA. Twenty-four hours after transfection, the luciferase substrate coelenterazine h (PerkinElmer) was added to achieve a final concentration of 5 μM to about 10^5 cells. Luminescence and fluorescence were measured simultaneously using the Mithras fluorescence-luminescence detector (Berthold) or Tecan Infinite 500. Filter sets 485 ± 10 nm and 530 ± 12.5 nm were used to detect luciferase emission and Venus emission, respectively. Luminescence and fluorescence values were corrected for coelenterazine h background emission on untransfected cells, and the ratio of fluorescence to luminescence was determined and compared to that of cells expressing donors alone.

Computational modeling

Computational models were built and simulated with the Simmune software, as described in the modeling supplement. The software is freely available (at https://exon.niaid.nih.gov/simmunereg/register.html) and can be downloaded without registration. All models are provided in the Supplementary Modeling File.

SUPPLEMENTARY MATERIALS

www.sciencesignaling.org/cgi/content/full/11/524/eaal1253/DC1

Fig. S1. Specificity, baseline, and kinetics of STAT activation downstream of γ_c cytokines.
Fig. S2. Expression kinetics of γ_c cytokine receptors as a function of TCR activation in vivo and in vitro.
Fig. S3. Responses in human T cells mimic those found in mouse T cells.
Fig. S4. STAT activation at different receptor occupancies for γ_c cytokines and determination of IL-7 and IL-4 dissociation constants.
Fig. S5. The cell surface abundance of γ_c is not affected by IL-4 or IL-7.
Fig. S6. Computational modeling reproduces experimentally determined cytokine dose-response curves and IL-7–induced suppression of IL-4–induced STAT6 phosphorylation.
Fig. S7. IL-7 signaling–induced phosphatase directed at STATs is not responsible for the inhibitory action of IL-7.
Table S1. Reported affinities of γ_c cytokines for their receptors.
Table S2. Parameter values used for simulating the affinity conversion model.
Table S3. Raw MFI values for receptor expression and calculated numbers of antibodies bound.
Supplementary Modeling File
Simmune modeling files
References (*52*–*63*)

REFERENCES AND NOTES

1. Y. Rochman, R. Spolski, W. J. Leonard, New insights into the regulation of T cells by γ_c family cytokines. *Nat. Rev. Immunol.* **9**, 480–490 (2009).
2. H. Yamane, W. E. Paul, Cytokines of the γ_c family control $CD4^+$ T cell differentiation and function. *Nat. Immunol.* **13**, 1037–1044 (2012).
3. C. M. Smyth, S. L. Ginn, C. T. Deakin, G. J. Logan, I. E. Alexander, Limiting γ_c expression differentially affects signaling via the interleukin (IL)-7 and IL-15 receptors. *Blood* **110**, 91–98 (2007).
4. M. Kondo, T. Takeshita, N. Ishii, M. Nakamura, S. Watanabe, K. Arai, K. Sugamura, Sharing of the interleukin-2 (IL-2) receptor gamma chain between receptors for IL-2 and IL-4. *Science* **262**, 1874–1877 (1993).
5. M. Noguchi, Y. Nakamura, S. M. Russell, S. F. Ziegler, M. Tsang, X. Cao, W. J. Leonard, Interleukin-2 receptor gamma chain: A functional component of the interleukin-7 receptor. *Science* **262**, 1877–1880 (1993).
6. S. M. Russell, A. D. Keegan, N. Harada, Y. Nakamura, M. Noguchi, P. Leland, M. C. Friedmann, A. Miyajima, R. K. Puri, W. E. Paul, W. J. Leonard, Interleukin-2 receptor gamma chain: A functional component of the interleukin-4 receptor. *Science* **262**, 1880–1883 (1993).
7. K. Nelms, A. D. Keegan, J. Zamorano, J. J. Ryan, W. E. Paul, The IL-4 receptor: Signaling mechanisms and biologic functions. *Annu. Rev. Immunol.* **17**, 701–738 (1999).
8. G. X. Masse, E. Corcuff, H. Decaluwe, U. Bommhardt, O. Lantz, J. Buer, J. P. Di Santo, γ_c cytokines provide multiple homeostatic signals to naive $CD4^+$ T cells. *Eur. J. Immunol.* **37**, 2606–2616 (2007).
9. D. M. Kemeny, The role of the T follicular helper cells in allergic disease. *Cell. Mol. Immunol.* **9**, 386–389 (2012).
10. M. A. Burke, B. F. Morel, T. B. Oriss, J. Bray, S. A. McCarthy, P. A. Morel, Modeling the proliferative response of T cells to IL-2 and IL-4. *Cell. Immunol.* **178**, 42–52 (1997).
11. A. Castro, T. K. Sengupta, D. C. Ruiz, E. Yang, L. B. Ivashkiv, IL-4 selectively inhibits IL-2-triggered Stat5 activation, but not proliferation, in human T cells. *J. Immunol.* **162**, 1261–1269 (1999).
12. K. Ozaki, R. Spolski, C. G. Feng, C.-F. Qi, J. Cheng, A. Sher, H. C. Morse III, C. Liu, P. L. Schwartzberg, W. J. Leonard, A critical role for IL-21 in regulating immunoglobulin production. *Science* **298**, 1630–1634 (2002).
13. J. H. Park, Q. Yu, B. Erman, J. S. Appelbaum, D. Montoya-Durango, H. L. Grimes, A. Singer, Suppression of IL7Rα transcription by IL-7 and other prosurvival cytokines: A novel mechanism for maximizing IL-7-dependent T cell survival. *Immunity* **21**, 289–302 (2004).
14. J. W. Cotari, G. Voisinne, O. E. Dar, V. Karabacak, G. Altan-Bonnet, Cell-to-cell variability analysis dissects the plasticity of signaling of common gamma chain cytokines in T cells. *Sci. Signal.* **6**, ra17 (2013).
15. M. J. Palmer, V. S. Mahajan, L. C. Trajman, D. J. Irvine, D. A. Lauffenburger, J. Chen, Interleukin-7 receptor signaling network: An integrated systems perspective. *Cell. Mol. Immunol.* **5**, 79–89 (2008).
16. T. Kitamura, N. Sato, K. Arai, A. Miyajima, Expression cloning of the human IL-3 receptor cDNA reveals a shared β subunit for the human IL-3 and GM-CSF receptors. *Cell* **66**, 1165–1174 (1991).

17. Y. Saito, T. Ogura, M. Kamio, H. Sabe, T. Uchiyama, T. Honjo, Stepwise formation of the high-affinity complex of the interleukin 2 receptor. *Int. Immunol.* **2**, 1167–1177 (1990).
18. C. A. McElroy, P. J. Holland, P. Zhao, J.-M. Lim, L. Wells, E. Eisenstein, S. T. R. Walsh, Structural reorganization of the interleukin-7 signaling complex. *Proc. Natl. Acad. Sci. U.S.A.* **109**, 2503–2508 (2012).
19. T. Rose, A.-H. Pillet, V. Lavergne, B. Tamarit, P. Lenormand, J.-C. Rousselle, A. Namane, J. Thèze, Interleukin-7 compartmentalizes its receptor signaling complex to initiate CD4 T lymphocyte response. *J. Biol. Chem.* **285**, 14898–14908 (2010).
20. S. Damjanovich, L. Bene, J. Matkó, A. Alileche, C. K. Goldman, S. Sharrow, T. A. Waldmann, Preassembly of interleukin 2 (IL-2) receptor subunits on resting Kit 225 K6 T cells and their modulation by IL-2, IL-7, and IL-15: A fluorescence resonance energy transfer study. *Proc. Natl. Acad. Sci. U.S.A.* **94**, 13134–13139 (1997).
21. N. I. Obiri, W. Debinski, W. J. Leonard, R. K. Puri, Receptor for interleukin 13. Interaction with interleukin 4 by a mechanism that does not involve the common γ chain shared by receptors for interleukins 2, 4, 7, 9, and 15. *J. Biol. Chem.* **270**, 8797–8804 (1995).
22. L. Swainson, S. Kinet, C. Mongellaz, M. Sourisseau, T. Henriques, N. Taylor, IL-7-induced proliferation of recent thymic emigrants requires activation of the PI3K pathway. *Blood* **109**, 1034–1042 (2007).
23. R. Tachdjian, S. Al Khatib, A. Schwinglshackl, H. S. Kim, A. Chen, J. Blasioli, C. Mathias, H. Y. Kim, D. T. Umetsu, H. C. Oettgen, T. A. Chatila, In vivo regulation of the allergic response by the IL-4 receptor α chain immunoreceptor tyrosine-based inhibitory motif. *J. Allergy Clin. Immunol.* **125**, 1128–1136.e8 (2010).
24. L. C. Osborne, S. Dhanji, J. W. Snow, J. J. Priatel, M. C. Ma, M. J. Miners, H.-S. Teh, M. A. Goldsmith, N. Abraham, Impaired CD8 T cell memory and CD4 T cell primary responses in IL-7Rα mutant mice. *J. Exp. Med.* **204**, 619–631 (2007).
25. R. G. Goodwin, D. Friend, S. F. Ziegler, R. Jerzy, B. A. Falk, S. Gimpel, D. Cosman, S. K. Dower, C. J. March, A. E. Namen, L. S. Park, Cloning of the human and murine interleukin-7 receptors: Demonstration of a soluble form and homology to a new receptor superfamily. *Cell* **60**, 941–951 (1990).
26. L. S. Park, D. J. Friend, A. E. Schmierer, S. K. Dower, A. E. Namen, Murine interleukin 7 (IL-7) receptor. Characterization on an IL-7-dependent cell line. *J. Exp. Med.* **171**, 1073–1089 (1990).
27. X. Wang, P. Lupardus, S. L. Laporte, K. C. Garcia, Structural biology of shared cytokine receptors. *Annu. Rev. Immunol.* **27**, 29–60 (2009).
28. A. Hémar, A. Subtil, M. Lieb, E. Morelon, R. Hellio, A. Dautry-Varsat, Endocytosis of interleukin 2 receptors in human T lymphocytes: Distinct intracellular localization and fate of the receptor α, β, and γ chains. *J. Cell Biol.* **129**, 55–64 (1995).
29. K. Kurgonaite, H. Gandhi, T. Kurth, S. Pautot, P. Schwille, T. Weidemann, C. Bökel, Essential role of endocytosis for interleukin-4-receptor-mediated JAK/STAT signalling. *J. Cell Sci.* **128**, 3781–3795 (2015).
30. I. Moraga, D. Richter, S. Wilmes, H. Winkelmann, K. Jude, C. Thomas, M. M. Suhoski, E. G. Engleman, J. Piehler, K. C. Garcia, Instructive roles for cytokine-receptor binding parameters in determining signaling and functional potency. *Sci. Signal.* **8**, ra114 (2015).
31. S. Kondo, A. Shimizu, Y. Saito, M. Kinoshita, T. Honjo, Molecular basis for two different affinity states of the interleukin 2 receptor: Affinity conversion model. *Proc. Natl. Acad. Sci. U.S.A.* **83**, 9026–9029 (1986).
32. B. R. Angermann, F. Klauschen, A. D. Garcia, T. Prustel, F. Zhang, R. N. Germain, M. Meier-Schellersheim, Computational modeling of cellular signaling processes embedded into dynamic spatial contexts. *Nat. Methods* **9**, 283–289 (2012).
33. H.-C. Cheng, B. R. Angermann, F. Zhang, M. Meier-Schellersheim, NetworkViewer: Visualizing biochemical reaction networks with embedded rendering of molecular interaction rules. *BMC Syst. Biol.* **8**, 70 (2014).
34. F. Zhang, B. R. Angermann, M. Meier-Schellersheim, The Simmune Modeler visual interface for creating signaling networks based on bi-molecular interactions. *Bioinformatics* **29**, 1229–1230 (2013).
35. S. J. Haque, Q. Wu, W. Kammer, K. Friedrich, J. M. Smith, I. M. Kerr, G. R. Stark, B. R. Williams, Receptor-associated constitutive protein tyrosine phosphatase activity controls the kinase function of JAK1. *Proc. Natl. Acad. Sci. U.S.A.* **94**, 8563–8568 (1997).
36. U. Klingmüller, U. Lorenz, L. C. Cantley, B. G. Neel, H. F. Lodish, Specific recruitment of SH-PTP1 to the erythropoietin receptor causes inactivation of JAK2 and termination of proliferative signals. *Cell* **80**, 729–738 (1995).
37. D. Xu, C. K. Qu, Protein tyrosine phosphatases in the JAK/STAT pathway. *Front. Biosci.* **13**, 4925–4932 (2008).
38. M. T. Kasaian, M. J. Whitters, L. L. Carter, L. D. Lowe, J. M. Jussif, B. Deng, K. A. Johnson, J. S. Witek, M. Senices, R. F. Konz, A. L. Wurster, D. D. Donaldson, M. Collins, D. A. Young, M. J. Grusby, IL-21 limits NK cell responses and promotes antigen-specific T cell activation: A mediator of the transition from innate to adaptive immunity. *Immunity* **16**, 559–569 (2002).
39. R. Zeng, R. Spolski, S. E. Finkelstein, S. Oh, P. E. Kovanen, C. S. Hinrichs, C. A. Pise-Masison, M. F. Radonovich, J. N. Brady, N. P. Restifo, J. A. Berzofsky, W. J. Leonard, Synergy of IL-21 and IL-15 in regulating $CD8^+$ T cell expansion and function. *J. Exp. Med.* **201**, 139–148 (2005).
40. S. L. LaPorte, Z. S. Juo, J. Vaclavikova, L. A. Colf, X. Qi, N. M. Heller, A. D. Keegan, K. C. Garcia, Molecular and structural basis of cytokine receptor pleiotropy in the interleukin-4/13 system. *Cell* **132**, 259–272 (2008).
41. T. Weidemann, R. Worch, K. Kurgonaite, M. Hintersteiner, C. Bökel, P. Schwille, Single cell analysis of ligand binding and complex formation of interleukin-4 receptor subunits. *Biophys. J.* **101**, 2360–2369 (2011).
42. A. Whitty, N. Raskin, D. L. Olson, C. W. Borysenko, C. M. Ambrose, C. D. Benjamin, L. C. Burkly, Interaction affinity between cytokine receptor components on the cell surface. *Proc. Natl. Acad. Sci. U.S.A.* **95**, 13165–13170 (1998).
43. H. B. Gaspar, K. L. Parsley, S. Howe, D. King, K. C. Gilmour, J. Sinclair, G. Brouns, M. Schmidt, C. Von Kalle, T. Barington, M. A. Jakobsen, H. O. Christensen, A. Al Ghonaium, H. N. White, J. L. Smith, R. J. Levinsky, R. R. Ali, C. Kinnon, A. J. Thrasher, Gene therapy of X-linked severe combined immunodeficiency by use of a pseudotyped gammaretroviral vector. *Lancet* **364**, 2181–2187 (2004).
44. S. Hacein-Bey-Abina, F. Le Deist, F. Carlier, C. Bouneaud, C. Hue, J.-P. De Villartay, A. J. Thrasher, N. Wulffraat, R. Sorensen, S. Dupuis-Girod, A. Fischer, E. G. Davies, W. Kuis, L. Leiva, M. Cavazzana-Calvo, Sustained correction of X-linked severe combined immunodeficiency by ex vivo gene therapy. *N. Engl. J. Med.* **346**, 1185–1193 (2002).
45. S. Hacein-Bey-Abina, C. von Kalle, M. Schmidt, F. Le Deist, N. Wulffraat, E. McIntyre, I. Radford, J. L. Villeval, C. C. Fraser, M. Cavazzana-Calvo, A. Fischer, A serious adverse event after successful gene therapy for X-linked severe combined immunodeficiency. *N. Engl. J. Med.* **348**, 255–256 (2003).
46. S. J. Howe, M. R. Mansour, K. Schwarzwaelder, C. Bartholomae, M. Hubank, H. Kempski, M. H. Brugman, K. Pike-Overzet, S. J. Chatters, D. de Ridder, K. C. Gilmour, S. Adams, S. I. Thornhill, K. L. Parsley, F. J. T. Staal, R. E. Gale, D. C. Linch, J. Bayford, L. Brown, M. Quaye, C. Kinnon, P. Ancliff, D. K. Webb, M. Schmidt, C. von Kalle, H. B. Gaspar, A. J. Thrasher, Insertional mutagenesis combined with acquired somatic mutations causes leukemogenesis following gene therapy of SCID-X1 patients. *J. Clin. Invest.* **118**, 3143–3150 (2008).
47. S. Amorosi, I. Russo, G. Amodio, C. Garbi, L. Vitiello, L. Palamaro, M. Adriani, I. Vigliano, C. Pignata, The cellular amount of the common γ-chain influences spontaneous or induced cell proliferation. *J. Immunol.* **182**, 3304–3309 (2009).
48. I. Vigliano, L. Palamaro, G. Bianchino, A. Fusco, L. Vitiello, V. Grieco, R. Romano, M. Salvatore, C. Pignata, Role of the common γ chain in cell cycle progression of human malignant cell lines. *Int. Immunol.* **24**, 159–167 (2012).
49. S. J. Orr, S. Roessler, L. Quigley, T. Chan, J. W. Ford, G. M. O'Connor, D. W. McVicar, Implications for gene therapy-limiting expression of IL-2Rγ_c delineate differences in signaling thresholds required for lymphocyte development and maintenance. *J. Immunol.* **185**, 1393–1403 (2010).
50. T. J. Crites, K. Padhan, J. Muller, M. Krogsgaard, P. R. Gudla, S. J. Lockett, R. Varma, TCR microclusters pre-exist and contain molecules necessary for TCR signal transduction. *J. Immunol.* **193**, 56–67 (2014).
51. T. J. Crites, L. Chen, R. Varma, A TIRF microscopy technique for real-time, simultaneous imaging of the TCR and its associated signaling proteins. *J. Vis. Exp.* 3892 (2012).
52. W. S. Hlavacek, J. R. Faeder, The complexity of cell signaling and the need for a new mechanics. *Sci. Signal.* **2**, pe46 (2009).
53. S. Joe, F. Y. Kuo, Remark on algorithm 659: Implementing Sobol's quasirandom sequence generator. *ACM Trans. Math. Softw.* **29**, 49–57 (2003).
54. N. P. Manes, B. R. Angermann, M. Koppenol-Raab, E. An, V. H. Sjoelund, J. Sun, M. Ishii, R. N. Germain, M. Meier-Schellersheim, A. Nita-Lazar, Targeted proteomics-driven computational modeling of macrophage S1P chemosensing. *Mol. Cell. Proteomics* **14**, 2661–2681 (2015).
55. X. Xu, T. Meckel, J. A. Brzostowski, J. Yan, M. Meier-Schellersheim, T. Jin, Coupling mechanism of a GPCR and a heterotrimeric G protein during chemoattractant gradient sensing in *Dictyostelium*. *Sci. Signal.* **3**, ra71 (2010).
56. I. P. Sugar, J. Das, C. Jayaprakash, S. C. Sealfon, Multiscale modeling of complex formation and CD80 depletion during immune synapse development. *Biophys. J.* **112**, 997–1009 (2017).
57. N. Harada, B. E. Castle, D. M. Gorman, N. Itoh, J. Schreurs, R. L. Barrett, M. Howard, A. Miyajima, Expression cloning of a cDNA encoding the murine interleukin 4 receptor based on ligand binding. *Proc. Natl. Acad. Sci. U.S.A.* **87**, 857–861 (1990).
58. B. Mosley, M. P. Beckmann, C. J. March, R. L. Idzerda, S. D. Gimpel, T. Vanden Bos, D. Friend, A. Alpert, D. Anderson, J. Jackson, J. M. Wignall, C. Smith, B. Gallis, J. E. Sims, D. Urdal, M. B. Widmer, D. Cosman, L. S. Park, The murine interleukin-4 receptor: Molecular cloning and characterization of secreted and membrane bound forms. *Cell* **59**, 335–348 (1989).
59. R. L. Idzerda, C. J. March, B. Mosely, S. D. Lyman, T. Vanden Bos, S. D. Gimpel, W. S. Din, K. H. Grabstein, M. B. Widmer, L. S. Park, D. Cosman, M. P. Beckmann, Human interleukin 4 receptor confers biological responsiveness and defines a novel receptor superfamily. *J. Exp. Med.* **171**, 861–873 (1990).
60. S. M. Grunewald, S. Kunzmann, B. Schnarr, J. Ezernieks, W. Sebald, A. Duschl, A murine interleukin-4 antagonistic mutant protein completely inhibits interleukin-4-induced cell proliferation, differentiation, and signal transduction. *J. Biol. Chem.* **272**, 1480–1483 (1997).

61. W. Lundström, S. Highfill, S. T. R. Waslsh, S. Beq, E. Morse, I. Kockum, L. Alfredsson, T. Olsson, J. Hillert, C. L. Mackall, Soluble IL7Rα potentiates IL-7 bioactivity and promotes autoimmunity. *Proc. Natl. Acad. Sci. U.S.A.* **110**, E1761–E1770 (2013).
62. C. A. McElroy, J. A. Dohm, S. T. R. Walsh, Structural and biophysical studies of the human IL-7/IL-7Rα complex. *Structure* **17**, 54–65 (2009).
63. J.-L. Zhang, D. Foster, W. Sebald, Human IL-21 and IL-4 bind to partially overlapping epitopes of common γ-chain. *Biochem. Biophys. Res. Commun.* **300**, 291–296 (2003).

Acknowledgments: We thank S. Durum, J. O'Shea, R. Germain, D. Margulies, E. Huseby, K. Laky, and T. Crites for critically reading the manuscript. We would also like to thank A. Singer, D. McVicar, H. Park, and V. Lazarevic for helpful discussions and advice. We thank E. Wan and W. Leonard for providing the STAT3$^{-/-}$ mice; Y. Furumoto, A. Laurence, and J. O'Shea for providing STAT5a$^{-/-}$ and STAT5b$^{-/-}$ mice; and H. Park for SOCS1$^{-/-}$ mice. We thank N. Ishi and K. Sugamura for providing the TUGm3 antibody and J. Milner and M. Lawrence for frozen human PBMCs. We thank V. Lazaveric and her colleagues for help with experiments. R.V. would like to thank P. Sharma for inspiring comments and V. K. Ramanujan and C. N. Chujor for help with experiments. **Funding:** This work was supported by the intramural research program of NIAID, NIH. **Author contributions:** Experiments were conducted by P.G., E.G., K.S., P.C., and R.V. and were designed by P.G., B.R.A., R.V., and M.M.-S. Simmune software was developed by B.R.A. and M.M.-S. Simmune software was used to perform simulations of models by B.R.A., M.M.-S., and R.V. P.G., B.R.A., R.V., and M.M.-S. performed data analysis and wrote the manuscript. **Competing interests:** The authors declare that they have no competing interests. **Data and materials availability:** The Simmune software is freely available to download at https://niaid.github.io/simmune/.

Submitted 30 September 2016
Resubmitted 20 March 2017
Accepted 16 March 2018
Published 3 April 2018
10.1126/scisignal.aal1253

Citation: P. Gonnord, B. R. Angermann, K. Sadtler, E. Gombos, P. Chappert, M. Meier-Schellersheim, R. Varma, A hierarchy of affinities between cytokine receptors and the common gamma chain leads to pathway cross-talk. *Sci. Signal.* **11**, eaal1253 (2018).